A Study of AR-, TS-, and MCS-Associated Precipitation and Extreme Precipitation in Present and Warmer Climates

Ming Zhao, *Geophysical Fluid Dynamics Laboratory/NOAA, Princeton, NJ, USA*

Motivation

- How much of the present-day climatological precipitation and extreme precipitation may be attributed to atmospheric rivers (ARs), tropical storms (TSs), and mesoscale convective systems (MCSs)?
- How well are AR, TS, and MCS associated precipitation and extreme precipitation simulated in the latest GFDL moderately high resolution (50km) GCM?
- How may AR, TS, and MCS associated precipitation change in a warmer climate?
- How may we understand the change in AR, TS, and MCS associated extreme precipitation in a warmer climate?

Observational data

- Precipitation: Multi-Source Weighted-Ensemble Precipitation (MSWEP-v2, Beck et al. 2019 BAMS, 1980-2014)
- Atmospheric Rivers: Integrated Vapor Transport from ERA-Interim reanalysis (1980-2014)
- Tropical Storms: International Best Track Archive for Climate Stewardship (IBTrACS) (1980-2014)
- Mesoscale Convective Systems: Multi-Satellite Infrared Brightness Temperature from CLoud Archive User Service (CLAUS) (1985-2008)

Model and simulations

- GFDL HighResMIP participating model: **C192AM4** (50km resolution) (Zhao 2020: AR, Murakami et al. 2020: TS, Dong et al. 2021: MCS)
- **PRESENT** (1980-2014): present-day simulation with C192AM4 forced by observed SSTs, SICs, radiative gases and aerosol emissions
- **CLIMO** (100 years): climatological simulation with C192AM4 forced by observed monthly varying climatological (1980-2014 average) SSTs and SICs with radiative gases and aerosol emissions fixed at 2010 condition
- **P4K** (100 years): As in CLIMO except with the SSTs increased uniformly by 4K

Storm detection methods

- Atmospheric Rivers (Guan & Waliser 2015, Zhao 2020)
  - Integrated Vapor Transport (IVT) Method, $IVT_{th} = \max(IVT^{85th}, 100\text{kg/m/s})$
  - Geometry requirement: Length ≥ 2000km, Length/Width ≥ 2
  - Poleward water transport ≥ 50 kg/m/s
  - Coherence of IVT direction ≥ 0.5
- Tropical Storms (Zhao et al. 2009, 2012)
  - Locate local maximums of 850-hPa relative vorticity exceeding a threshold
  - Define their nearby local minimum of SLP as cyclone centers
  - Track individual TCs using 6-hourly cyclone locations
  - Check track with criteria (maximum windspeed, relative vorticity, warm-core, duration)
  - 12˚x12˚ centered at each TC center considered as TS region
- Mesoscale Convective Systems (Dong et al. 2021, Huang et al. 2018)
  - Derive Brightness temperature (T_b) using OLR (Ellingson and Ferraro 1983)
  - Remove grid cells with $T_b(\lambda,\phi,t) \geq 233$ K and $T_b(\lambda,\phi,t) \geq T_b(\lambda,\phi,t)$-30 K
- AR, TS and MCS days
  - For a given grid cell and calendar day if at least one AR/TS/MCS condition identified from 6-hrly data and daily precipitation ≥ 1mm/day
  - Priority for overlap conditions: 1) TS → 2) AR→ 3) MCS (mutually exclusive)

Results

The global and annual mean frequency of AR, TS, and MCS days are respectively 8.33% (7.58%), 0.72% (0.99%) and 4.28% (4.37%) from the observations (model). Together they amount to roughly 13%, which is about 1/3 of the frequency of all wet days (P>1mm/day). While they may be considered relatively rare events globally, they occur more frequently regionally. The model shows significant regional biases over various regions (e.g. overestimate TCs over the W. Pacific and underestimate TCs over the E. Pacific and N. Atlantic).

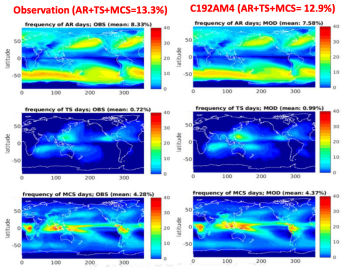

Fig. 1: Annual occurrence frequency of AR, TS, and MCS days (%)

Paper published in Journal of Climate DOI:10.1175/JCLI-D-21-0145.1

AR, TS, and MCS associated precipitation in present climate

Despite their occasional occurrence (~13%) globally, Fig. 2 shows that the AR, TS and MCS days together account for over 50% of the global annual mean precipitation in both the observations and the model. Individually, AR, TS and MCS days account for respectively 25% (24%), 4.1% (5.8%), and 24% (25%) of the global annual mean precipitation in the observations (model). Regionally, AR, TS and MCS associated precipitation can each contribute up to 50-60% of local annual precipitation. The model's biases in AR/TS/MCS associated precipitation are due to its biases in both storm frequency and intensity.

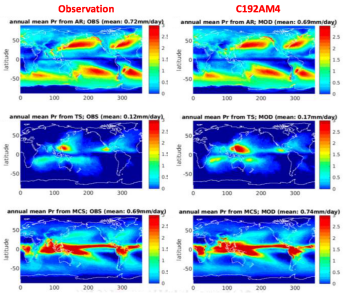

Fig. 2: Annual mean precipitation from AR, TS, and MCS days

Fig 3 shows that roughly 50-60% of annual precipitation over the NH and SH mid-latitude storm track regions are from the AR days. In parts of the eastern or western Pacific MDR regions, TSs can contribute up to 40-50% their local annual precipitation. In many parts of the deep tropics, the MCS days account for 50-60% of their annual precipitation. The model broadly captures the observed regional distribution of precipitation that is associated with AR, TS, and MCS days with a slight global underestimate (overestimate) of the AR (TS and MCS) precipitation.

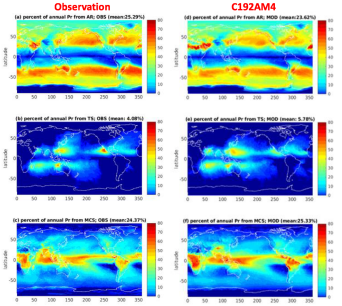

Fig. 3: Percent of annual precipitation from AR, TS, and MCS days

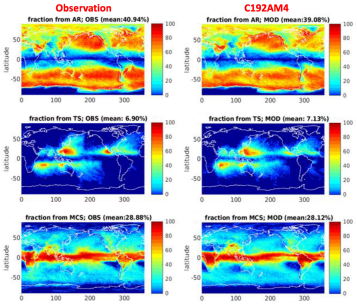

Fig. 4: Percent of extreme daily precipitation events (local 1% heaviest daily precipitation) from AR, TS, and MCS days

To quantify the contribution of ARs, TSs, and MCSs to daily precipitation extremes, Fig. 4 shows the fraction of local 1% heaviest daily precipitation events that come from AR, TS, and MCS days. Globally, the AR, TS and MCS days together account for ~75% of extreme precipitation. Regionally, these weather phenomena together account for 80-100% of extreme precipitation over most parts of the world. The model reproduces well the observed frequency of AR/TS/MCS associated extreme daily precipitation.

The model also reasonably well reproduces the observed AR/TS/MCS mean precipitation intensity. However, not all AR/TS/MCS days are equal. The AR/TS/MCS precipitation intensity tends to be dominated by the 25% heaviest-precipitation days, which produce a mean intensity 2-3 (10-20) times larger than that averaged over all AR/TS/MCS days (the 25% lightest-precipitation AR/TS/MCS days) (see paper). This suggests that the distribution of daily precipitation among the AR, TS and MCS days is strongly positively skewed, with their 25% heaviest-precipitation days playing the dominant role in both mean and extreme precipitation in the present climate.

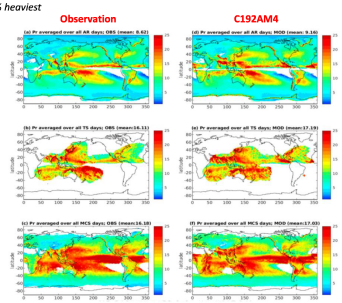

Fig. 5: Precipitation intensity averaged from all AR, TS, and MCS days.

AR, TS, and MCS associated precipitation change in a warmer climate

Fig. 6 shows that globally the model produces roughly a 2.85%/K increase in global mean precipitation, of which roughly 66% comes from the AR, TS, and MCS days. Individually, the AR, TS, and MCS associated global mean precipitation increases by 5.4%/K, 1.5%/K, and 2%/K respectively. The spatial distribution of changes in annual precipitation is well captured by the total changes in AR, TS and MCS associated precipitation with the net changes being dominated by the AR days in the middle and high latitude and by the TS and MCS days in the tropical and sub-tropical regions.

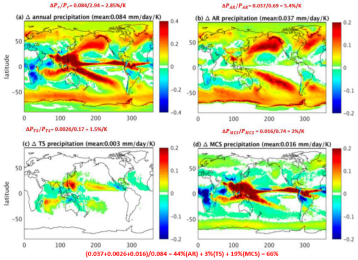

Fig. 6: Change in annual mean precipitation between P4K and CLIMO and its contributions from AR, TS, and MCS days

Fig. 7 shows that the spatial patterns of changes in AR/TS/MCS associated precipitation correlate well with their changes in frequency. Globally, the frequency of AR days increases slightly while the frequency of TS and MCS days decreases. Regionally, the maximum frequency of AR days tends to migrate poleward while the frequency of TS days increases over the central Pacific and part of the south Indian Ocean with a decrease elsewhere. The frequency of MCS days tends to increase over parts of the equatorial western and eastern Pacific warm pools and decrease over most parts of the tropics and subtropics. The percentage change in daily precipitation rate averaged over all AR/TS/MCS days increases relatively uniformly around the globe which is in sharp contrast with their changes in frequency.

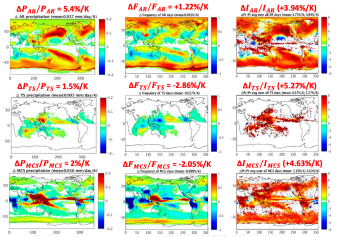

Fig. 7: Change in annual frequency of AR/TS/MCS days and the percentage change in precipitation intensity averaged over all AR/TS/MCS days

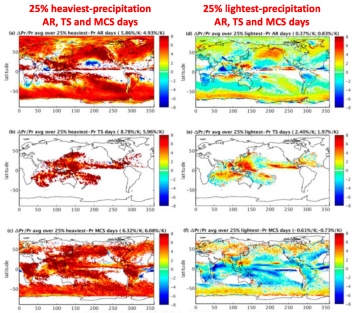

Fig. 8: Change in precipitation intensity averaged over the 25% heaviest-precipitation vs the 25% lightest-precipitation AR, TS, and MCS days

Fig 8. shows that the 25% heaviest-precipitation AR/TS/MCS days display a similar/larger percentage increase in precipitation intensity compared to the change in AR/TS/MCS mean precipitation intensity. In contrast, the 25% lightest-precipitation AR/TS/MCS days exhibit a much smaller increase or even a decrease in many regions.

Fig 9. further displays a decomposition of the precipitation change in 25% heaviest-precipitation AR/TS/MCS days into the dynamical and thermodynamic components. The result indicates the thermodynamic component is the primary cause of the increase in AR/TS/MCS associated mean precipitation intensity.

$$\Delta P_r/P_r \approx \Delta\omega_{500}/\omega_{500} + \Delta q_{850}/q_{850} + \Delta\varepsilon/\varepsilon$$

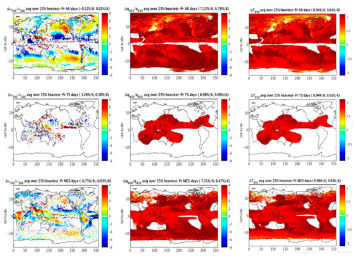

Fig. 9: Change in dynamic and thermodynamic environment averaged over the 25% heaviest-precipitation AR, TS, and MCS days.

Summary

Despite their occasional occurrence globally, AR, TS, and MCS days together account for ~55% of global mean precipitation and ~75% of extreme precipitation with daily rates exceeding its local 99th percentile. GFDL C192AM4 reproduces well the observed percentage of mean and extreme precipitation associated with AR, TS, and MCS days. In an idealized global warming simulation, the modeled changes in global mean and regional distribution of precipitation correspond well with changes in AR/TS/MCS precipitation. Globally, the frequency of AR days increases slightly while the frequency of TS and MCS days decreases. The AR/TS/MCS mean precipitation intensity increases by ~5%/K due primarily to precipitation increases in the top 25% of AR/TS/MCS days with the heaviest precipitation, which are dominated by the thermodynamic component with the dynamic and microphysical components playing a secondary role.